



# Photophysical and electrochemical redox properties of fixed distance porphyrin–quinone systems

Avijit Sen, V. Krishnan<sup>1,\*</sup>

*Department of Inorganic and Physical Chemistry, Indian Institute of Science, Bangalore 560 012, India*

Received 13 June 1998; received in revised form 28 December 1998; accepted 3 February 1999

## Abstract

A few fixed distance covalently linked porphyrin–quinone molecules have been synthesized in which a benzoquinone is directly attached to a *meso*/ $\beta$ -pyrrole position of tri(phenyl/pentafluorophenyl)/tetraphenylporphyrins. The choice of fluoroarylporphyrins permit modulation of  $\Delta G_{ET}$  values for photoinduced electron-transfer reactions in these systems. All short distance porphyrin–quinone molecules showed efficient quenching of the porphyrin singlet excited state. The electrochemical redox data coupled with the steady-state and time-resolved singlet emission data are analysed to evaluate the dependence of  $\Delta G_{ET}$  values on the rate of electron transfer ( $k_{ET}$ ) in these systems. The *meso*-trifluoroarylporphyrin–quinones are found to be sensitive probes of the surrounding dielectric environment. Varying solvent polarity on the mechanism of fluorescence quenching and  $k_{ET}$  values revealed that short donor–acceptor distance and the solvent dielectric relaxation properties play a dominant role. © 1999 Elsevier Science S.A. All rights reserved.

**Keywords:** Porphyrin–quinone systems; Time-resolved studies; Electron transfer; Redox-properties

## 1. Introduction

There has been a great deal of recent research on the properties of porphyrin containing molecular assemblies in an attempt to mimic the primary light-driven step in natural photosynthesis [1–3]. The covalently linked porphyrin–quinone molecules have attracted considerable attention to evolve an understanding of the critical role of variables such as distance, orientation, energetics and the role of the solvent medium to influence the rates of intramolecular electron transfer in these systems.

Most of the studies have concentrated on porphyrin–spacer–quinone systems with relatively long flexible covalent link(s) possessing various geometries and degrees of rigidity [2,4]. It is recognised in a few model studies that an important factor affecting the rates of forward ET and charge recombination reaction rests on the ability of the donor and acceptor moieties to assume one or more optimum configurations. Thus, there is a need to study DA systems comprising of rigid covalent linkages. All those studies are related to engineer the possible mechanistic details of

PET reactions on the DA distance and their optimum orientations [5,6]. However, vibrational degrees of freedom within the link, can give rise to distributions of ET rates and therefore there is a necessity for studies in the ultra short time scale [7,8]. There were reports on a porphyrin–quinone (PQ) molecule in which conformational freedom was minimised by covalently linking a benzoquinone directly at a *meso*-position of the triphenylporphyrin ring. A similar concept was reported in the study of *meso*-linked zinc porphyrin–anthroquinone by Kamioka et al. [9]. Photophysical studies on porphyrin–quinone systems showed a very rapid decay (<6 ps) of the porphyrin excited singlet state ( $S_1$ ) [10]. The transient absorption profile was attributed to the formation of charge separated (CT) state by both singlet and triplet mechanisms, and reverse ET from a vibrationally unrelaxed triplet charge separated state was postulated. It is likely that some of this complex behaviour arise from the relatively large driving force for forward electron transfer ( $\Delta G_{ET} \approx 420$  meV), which places the energy of the CT state very close to that of the localised porphyrin triplet state. There exists different ways in which the energy of the CT state can be modulated in the P–Q systems. The choice of systems arise (i) by linking diverse quinones with varying reduction potentials to the porphyrin, (ii) by altering the site, peripheral positions of the porphyrin, to which the quinone is covalently attached, and (iii) by changing the nature of the

\*Corresponding author. Tel.: +91-80-3092296; fax: +91-80-3341683; e-mail: vkrpic@postoffice.iisc.ernet.in

<sup>1</sup>Also at Jawaharlal Nehru Centre for Advanced Scientific Research, Jakkur, Bangalore 560 012, India.

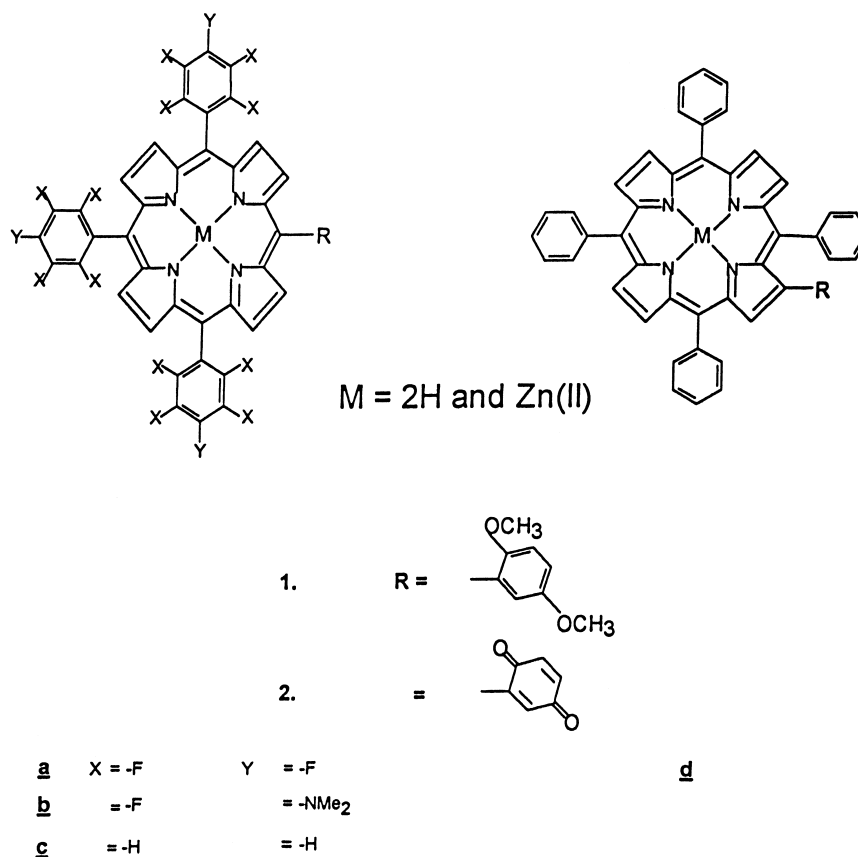


Fig. 1. The structure of the synthesized porphyrins.

porphyrin in the PQ systems so as to alter the first ring oxidation potential. It is found that pentafluorophenylporphyrins are more difficult to oxidise than tetraphenylporphyrin by  $\approx 500$  mV, hence a system containing a pentafluorophenylporphyrin coupled with a benzoquinone has an advantage for having less favourable energetics for ET and complications due to triplet mechanisms may not arise. These porphyrin–quinone systems might yield information on the relative importance of differences in Gibbs free-energy of charge separation. The detailed photophysical behaviour in such systems may be simpler as well.

In this report, we present the spectral and electrochemical properties of fixed distance porphyrin–quinone systems where a *p*-benzoquinone (BQ) is directly attached to the *meso*-carbon atom of fluoroarylporphyrins and in another, quinone moiety is directly attached to one of the  $\beta$ -pyrrole carbon atoms of a *meso*-tetraphenylporphyrin (Fig. 1). The possibility of having quinone moiety at the  $\beta$ -pyrrole carbon atom was considered to bring forth the difference in electronic ground state ( $a_{1u}/a_{2u}$ ) of the porphyrin as a consequence of *meso*- or  $\beta$ -substituent on the electron-transfer kinetics. Despite the availability of electron-transfer rate data [7,11,12] on porphyrin–quinone model systems for fairly large distances ranging from  $10.5^\circ$  to  $18.8 \text{ \AA}$  (center-to-center), information on the porphyrin–quinone systems with short ( $6.5 \text{ \AA}$ ) center-to-center distance is relatively

unknown. It is of interest to evaluate the effect of thermodynamic driving force on electron-transfer rate in these systems containing the acceptor at a fixed distance in different porphyrins. Here, we describe results of steady-state and time-resolved fluorescence studies of two fluoroarylporphyrins in which a benzoquinone is directly attached through a *meso*-carbon atom.

## 2. Experimental

All the chemicals used were procured from Fluka Chemicals (Switzerland) and used as received. The solvents employed in this study were distilled before use. The precursor porphyrin 5,10,15-tri(pentafluoro)phenyl-20(2,5-dimethoxy)phenylporphyrin ( $H_21a$ ) was synthesised by condensing pyrrole and respective benzaldehydes in appropriate ratio following the Lindsey procedure [13]. The desired compound 5,10,15-tri(pentafluoro)phenyl-20(*p*-benzoquinone) porphyrin ( $H_2a$ ) was obtained by demethylation of dimethoxy compound using  $BBr_3$  followed by oxidation with  $PbO_2$  [14]. 5,10,15-tri(2,3,5,6-tetrafluoro-4-dimethylamino) phenyl-20(2,5-dimethoxy)phenylporphyrin was synthesized from  $H_21a$  by nucleophilic substitution reaction as described earlier [15]. The corresponding quinone ( $H_22b$ ) was obtained by  $BBr_3$  demethylation reaction followed by

oxidation with  $\text{PbO}_2$ . The *meso*- and  $\beta$ -pyrrole-substituted porphyrins were synthesized as described earlier [10,14]. The zinc(II) derivatives of all the compounds were prepared by refluxing the respective porphyrin with zinc(II) acetate in  $\text{CHCl}_3$  and methanol mixture. All the compounds were purified by silica–gel column chromatography. Compounds were characterised by UV-VIS,  $^1\text{H}$ ,  $^{19}\text{F}$ -NMR and FAB-MS spectroscopies. Efforts were taken to avoid the contamination due to hydroquinone impurities in the samples for photophysical studies. Freshly chromatographed compounds under dark was used for all the studies.

The cyclic voltammograms and differential pulse voltammograms (DPV) were recorded on a BAS 100A Electrochemical Analyser. A three electrode assembly consisting of a gold working electrode was used for redox potential measurements. Dichloromethane was used as the solvent and  $\text{TBAPF}_6$  was used as the supporting electrolyte.

The spectrophotometers employed in this study were the same as described earlier [16]. The singlet excited state decay measurements were carried out using a picosecond laser excitation, time-correlated, single-photon counting method with the experimental apparatus described earlier [17]. The full width at half maximum (FWHM) of the instrument response function is typically 80–100 ps using a micro-channel photomultiplier (Hamamtsu R2809). Fluorescence decays were obtained at the magic angle ( $54.7^\circ$ ). The porphyrins were excited at 580 nm and emission was detected at different wavelengths depending on the emission peak positions of the porphyrins. All the decays were fitted

to single or bi-exponential equations convoluted by the instrument response function by the non-linear least-square method described earlier [18]. The ‘good fit’ criteria were a low  $\chi^2$  values (1.0–1.3) and random distributions of the residual. The samples were chromatographed and checked (by NMR) for purity prior to spectral studies.

### 3. Results and discussion

#### 3.1. Electrochemistry

The electrochemical redox measurements of differently linked porphyrin–quinone systems (Fig. 1) are analysed to probe into the effect induced by quinone (located at different peripheral positions of the porphyrins) on the  $\Delta G_{\text{ET}}$  values. All the potentials reported here are relative to internal  $\text{Fc}^+/\text{Fc}$  couple. The cyclic voltammetry of 1,4-benzoquinone in  $\text{CH}_2\text{Cl}_2$  carried out under the same conditions of measurements display two neat one-electron reversible reduction steps at  $-925$  and  $-1395$  mV, respectively. The electrochemical data of the porphyrins are summarised in Table 1 along with  $\Delta G_{\text{ET}}$  values. These  $\Delta G_{\text{ET}}$  values are uncorrected for coulomb interactions in the charge separated state and ion-pairing effects in the electrochemical measurements. The data on non-quinonoid dimethoxybenzeneporphyrin systems are useful in the identification of first ring reduction potential of the porphyrin since this often overlaps with the second reduction potential of the quinone in the

Table 1  
Electrochemical redox data <sup>a</sup> (in mV) of the porphyrins in  $\text{CH}_2\text{Cl}_2$  at 300 K

Compound	$\text{P}^{+\cdot}$	$\text{P}^{+2}$	$\text{Q}_1$	$\text{Q}_2$	$\text{P}^{\cdot-}$	$\text{P}^{-2}$	$-\Delta G_{\text{ET}}^{\text{b}}$ (meV)
$\text{H}_2\text{1a}$	910	1100	—	—	-1360	-1770	—
$\text{H}_2\text{1b}$	750	970	—	—	-1460	-1875	—
$\text{H}_2\text{1c}$	525	845	—	—	-1680	-2000	—
$\text{H}_2\text{1d}$	490	720	—	—	-1700	-1990	—
$\text{H}_2\text{2a}$	1030	— <sup>c</sup>	-800	-1370	-1470	-1790	100
$\text{H}_2\text{2b}$	855	— <sup>c</sup>	-810	-1390	-1560	-1865	245
$\text{H}_2\text{2c}$	625	910	-860	-1450	-1740	-2010	415
$\text{H}_2\text{2d}$	560	765	-990	-1515	-1675	— <sup>d</sup>	360
$\text{Zn1a}$	710	950	—	—	-1520	-1940	—
$\text{Zn1b}$	600	810	—	—	-1615	-2020	—
$\text{Zn1c}$	355	640	—	—	— <sup>d</sup>	— <sup>d</sup>	—
$\text{Zn1d}$	345	600	—	—	— <sup>d</sup>	— <sup>d</sup>	—
$\text{Zn2a}$	780	1020	-690	-1400	-1820	-2010	650
$\text{Zn2b}$	670	— <sup>c</sup>	-725	-1390	-1900	-2030	730
$\text{Zn2c}$	430	710	-800	— <sup>c</sup>	— <sup>d</sup>	— <sup>d</sup>	860
$\text{Zn2d}$	385	660	-970	— <sup>c</sup>	— <sup>d</sup>	— <sup>d</sup>	725
<i>p</i> -Benzoquinone (BQ)	—	—	-925	-1395	—	—	—
(BQ) + $\text{H}_2\text{1a}$ (1 : 1 mix)	910	1100	-920	—	-1370 <sup>e</sup>	-1770	—
(BQ) + $\text{H}_2\text{1b}$ (1 : 1 mix)	750	965	-930	—	-1420 <sup>e</sup>	-1870	—

<sup>a</sup> The potentials are referenced against  $\text{Fc}/\text{Fc}^+$  (0.0 V).

<sup>b</sup> Was obtained from the relation,  $\Delta G_{\text{ET}} = \text{P}^{+\cdot} - \text{Q}_1 - \Delta E_{(0,0)}$  is  $S_0 \rightarrow S_1$  excitation energy.

<sup>c</sup> Not observed or too close to solvent redox potential.

<sup>d</sup> Irreversible.

<sup>e</sup> Overlapped with quinone second reduction; Uncertainty in redox potential is  $\pm 15$  mV.

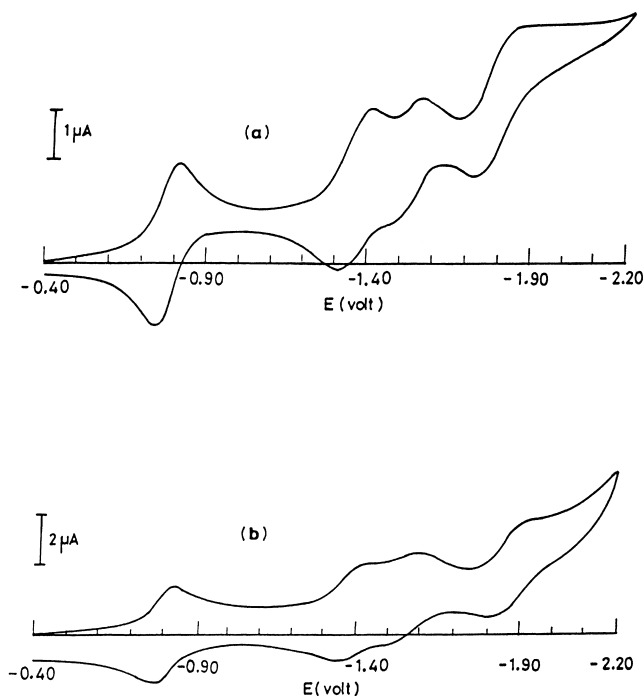


Fig. 2. Cyclic voltammograms of free-base fluoroarylporphyrin-quinones (a) H<sub>2</sub>2a, and H<sub>2</sub>2b in CH<sub>2</sub>Cl<sub>2</sub> solution containing 0.1 M TBAPF<sub>6</sub> at 300 K.

corresponding porphyrin-quinone systems. Typical cyclic voltammograms of two free-base *meso*-fluoroarylporphyrin-quinone systems are displayed in Fig. 2. Two effects are followed from the electrochemical measurements (Table 1): (i) the shift in the porphyrin ring redox potentials (45–120 mV) as a result of quinone substitution at the pyrrole and *meso*-carbons of the porphyrin; and (ii) the shift in the first reduction potential (50–240 mV) of the quinone as a consequence of its proximity to the porphyrin. In general, an anodic shift of the ring oxidation potential (relative to the corresponding dimethoxybenzene derivatives) is observed in the porphyrin-quinone systems. The shift in the potential is well pronounced ( $\approx 100$  mV) in the first ring oxidation of the porphyrin while  $\approx 60$  mV shift is observed in the second ring oxidation. The porphyrin ring reductions in a few cases are found to be irreversible, however, these occur at a more cathodic potential relative to the corresponding dimethoxybenzene analogues. It was noted that the presence of a quinone in the *meso*-position of the porphyrin results in substantive shift in the ring oxidation potential relative to that observed for the  $\beta$ -substituted quinone derivatives. Let us turn our attention to the quinone reductions for free-base tri/tetraphenylporphyrin-quinone systems. The effect of the *meso*-substitution clearly results in the reduction of quinone to a more anodic potential ( $-860$  mV) while the  $\beta$ -substitution leads to a more cathodic potential ( $-980$  mV) relative to the reduction potential of the unbound quinone at  $-925$  mV. Similar trend was observed for the corresponding zinc(II) derivatives. The data in Table 1 also shows that for all the *meso*-substituted

porphyrin-quinone systems there was an anodic shift for the first reduction of the attached quinone relative to the unbound quinone. Interestingly, the effect of zinc(II) ion in the porphyrin was found to be more in the first reduction of the quinone at *meso*-carbon than that of  $\beta$ -pyrrole linked quinone. These results suggest that the energy of the CT states ( $P^{+}Q^{-}$ ) are distinguishable in the *meso*- and  $\beta$ -pyrrole-substituted porphyrin-quinone systems which in turn, governs the  $\Delta G_{ET}$  values. The presence of fluoroaryl groups in the porphyrin shifts the ring oxidations to a more anodic potentials ( $\approx 400$  mV) relative to that observed for corresponding tri/tetraphenylporphyrin and hence reduce the thermodynamic driving force for electron transfer ( $\Delta G_{ET}$ ) to a considerable amount (Table 1). As pointed out earlier [19], the introduction of electron donating –NMe<sub>2</sub> groups in the *meso*-fluoroaryl rings shift both the ring centered redox potentials cathodically by ca. 100–150 mV, leaving the first reduction potential of the quinone almost unaltered. These systems provide a convenient method for assignments of the redox potentials in fluoroarylporphyrin-quinones and in fine-tuning the  $\Delta G_{ET}$  values in these systems.

### 3.2. Absorption spectroscopy

The optical absorption spectra of the free-base porphyrin-quinones and corresponding dimethoxybenzene derivatives showed very characteristic  $\pi-\pi^*$  electronic transitions with a strong Soret band in the region 410–420 nm ( $\epsilon \sim 10^5$  M<sup>-1</sup> cm<sup>-1</sup>) of the allowed  $S_0-S_2$  transition and different components of Q bands ( $S_0-S_1$  transition) between 500 and 650 nm. Typical absorption spectra of the quinonoid and non-quinonoid free-base derivative are displayed in Fig. 3. The absorption data of the free-base porphyrin-quinones and their zinc(II) derivatives, with their non-quinonoid analogues are summarised in Tables 2 and 3, respectively. The absorption spectra of the quinone compounds are almost identical with that of non-quinonoid porphyrins except for the absorbance of the quinone subunit in the region of 248 nm. The Soret band was found to be blue shifted by 2–3 nm and the Q<sub>x</sub>(0,0) band was red shifted by  $\sim 4$  nm in porphyrin-quinones relative to the respective non-quinonoid compounds. There was a marginal difference in the absorption coefficients ( $\epsilon$  values) and full width at half maxima (FWHM) values of  $\pi-\pi^*$  transitions of porphyrin bands in the porphyrin-quinones compared to that observed for the dimethoxybenzene derivatives. The small shift in the absorption bands and change in the absorption coefficients with reference to dimethoxy compounds probably results from the difference in electronic nature of benzoquinone and dimethoxybenzene substituted at the *meso*/ $\beta$ -position of the porphyrin macrocycle. This is similar to those reported for the *meso*-substituted octaalkylporphyrins [20]. It is ascribed to the different angular interactions between the electrons of the bulky *meso*-substituent (BQ) and the  $\pi$ -orbitals of the porphyrin of ( $a_{2u}/a_{1u}$ ) symmetry with electron density loca-

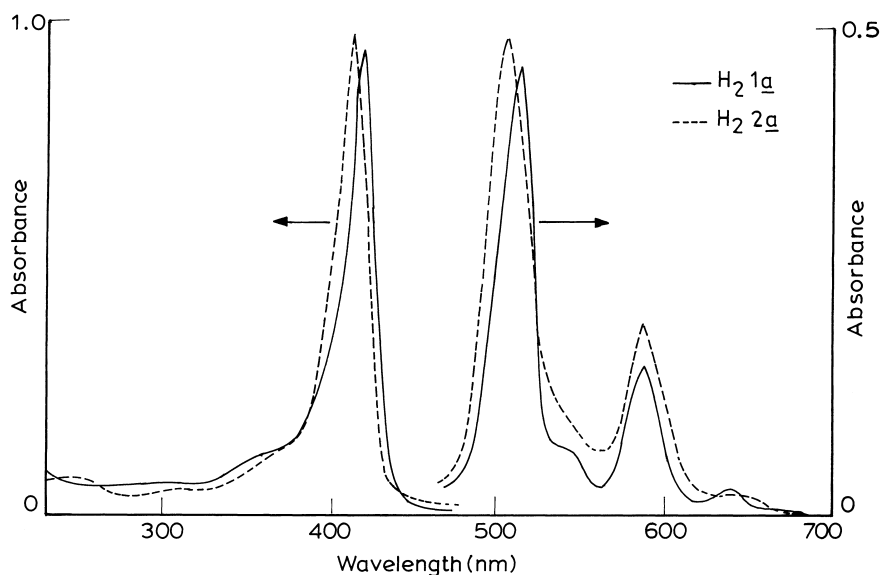


Fig. 3. Absorption spectra of the free-base fluoroarylporphyrins in  $\text{CH}_2\text{Cl}_2$  solution at 300 K non-quinonoid ( $\text{H}_2\text{1a}$ ) and porphyrin–quinone ( $\text{H}_2\text{2a}$ ).

lised on the pyrrole carbons which leads to the perturbation of the  $Y$  component of the absorption bands [21]. The absence of any strong ground-state interaction between the porphyrin unit and the attached quinone moiety has earlier been pointed out [14].

### 3.3. Fluorescence

The fluorescence spectra of the porphyrin–quinones exhibit two emission bands similar to that observed for non-quinonoid *meso*-tetraarylporphyrins. The representative

fluorescence spectra of free-base porphyrin–quinones and their dimethoxybenzene analogues in dichloromethane solution are shown in Fig. 4. The emission maxima and the relative quantum yields in the same solvents are listed in Table 4 along with the corrected  $\Delta G_{\text{ET}}$  values which incorporates both the solvent-dependent coulomb energy change upon ion-pair formation or recombination and the free energy of solvation of the ions applying Weller's equation [12,22].

We are not able to observe any fluorescence emission for the zinc(II) derivatives of *meso*-tri/tetraphenylporphyrin–

Table 2  
Optical absorption and fluorescence data of the free-base porphyrins in  $\text{CH}_2\text{Cl}_2$  at 300 K

Compound	Quinone	Bands (nm) <sup>a</sup>					$\lambda_{\text{em}}$ <sup>b</sup> (nm)
		soret	$Q_y(1,0)$	$Q_y(0,0)$	$Q_x(1,0)$	$Q_x(0,0)$	
$\text{H}_2\text{1a}$		414 (5.46,1111)	510 (4.32,539)	542 (3.51,539)	585 (3.84,584)	639 (3.06,— <sup>d</sup> )	636,705 (1.0)
	247 (4.46,— <sup>d</sup> )	411 (546,1126)	508 (4.26,583)		586 (3.81,608)	639 (2.94,— <sup>d</sup> )	643,707 ( $1.6 \times 10^{-3}$ )
$\text{H}_2\text{2a}$	268	420	512	545	587	647	648711
	(4.48,— <sup>d</sup> )	(5.44,1196)	(4.32,803)	(3.72,— <sup>d</sup> )	(3.84,579)	(3.18,— <sup>d</sup> )	(1.0)
$\text{H}_2\text{2b}$	257	417	510	544(sh)	589	646	654,710
	(4.57,— <sup>d</sup> )	(5.34,1265)	(4.21,962)	(3.69,— <sup>d</sup> )	(3.80,632)	(3.07,— <sup>d</sup> )	(0.08)
$\text{H}_2\text{2c}$		418		549	589	645	648,709
		(5.33,715)		(375,465)	(3.64,539)	(3.44,365)	(1.0)
$\text{H}_2\text{2c}$	249	416	511	544	590	649	649,710
	(4.30,— <sup>d</sup> )	(5.60,797)	(4.22,837)	(2.74,— <sup>d</sup> )	(3.78,659)	(3.53,573)	(< $10^{-3}$ )
$\text{H}_2\text{1d}$		420	517	552	592	647	653,716
		(5.50,794)	(4.20,744)	(3.77,493)	(3.67,570)	(3.45,406)	(1.0)
$\text{H}_2\text{1d}$	249	420	518	550	595	653	653,716
	(4.21,— <sup>d</sup> )	(539,796)	(4.05,781)	(3.60,— <sup>d</sup> )	(3.52,623)	(3.52,623)	(< $10^{-3}$ )

<sup>a</sup>  $\log \epsilon$  and FWHM ( $\text{cm}^{-1}$ ) values are in parenthesis.

<sup>b</sup>  $\lambda_{\text{ex}} = 510$  nm,  $\phi$  values are in parenthesis.

<sup>c</sup> Non-fluorescent.

<sup>d</sup> For weak bands FWHM were not calculated.

Table 3  
Optical absorption and fluorescence data of zinc(II) derivatives of the porphyrins in CH<sub>2</sub>Cl<sub>2</sub> at 300 K

Compound	Quinone	Bands <sup>a</sup> (nm)			$\lambda_{em}$ <sup>b</sup> (nm)
		soret	Q(1,0)	Q(0,0)	
Zn1a		415(5.58,755)	545(4.31,708)	578(3.61,421)	587,639(1.0)
Zn2a	248(4.46,— <sup>d</sup> )	413(5.67,703)	547(4.27,771)	579(3.70,— <sup>d</sup> )	588,640(<10 <sup>-3</sup> )
Zn1b	263(4.48,— <sup>d</sup> )	421(5.58,963)	547(4.35,704)	579(3.44,— <sup>d</sup> )	588,642(1.0)
Zn2b	257(4.57,— <sup>d</sup> )	418(5.51,969)	547(4.24,830)	589,640(<10 <sup>-3</sup> )	
Zn1c		419(5.63,569)	548(4.27,689)	585(3.54,497)	596,650(1.0)
Zn2c	248	417(5.74,536)	546(4.25,842)		— <sup>c</sup>
Zn1d		423(5.58,728)	551(4.24,725)	590(3.45,497)	600,648(1.0)
Zn2d	251(4.31,— <sup>d</sup> )	421(5.68,677)	551(4.24,760)	590(3.62,— <sup>d</sup> )	600,648(1.0)

<sup>a</sup> log  $\epsilon$  and FWHM (cm<sup>-1</sup>) values are in parenthesis.

<sup>b</sup>  $\lambda_{ex}$  = 540 nm,  $\phi$  values are in parenthesis.

<sup>c</sup> Non-fluorescent.

<sup>d</sup> For weak bands FWHM values were not calculated.

quinone systems, however the corresponding fluoroarylporphyrin–quinones display weak fluorescence as shown in Fig. 5. The fluorescence quantum yields of non-quinonoid

dimethoxyphenylporphyrins are of the same order of magnitude as of those obtained for the corresponding *meso*-tetraarylporphyrins, while a drastic quenching of the fluor-

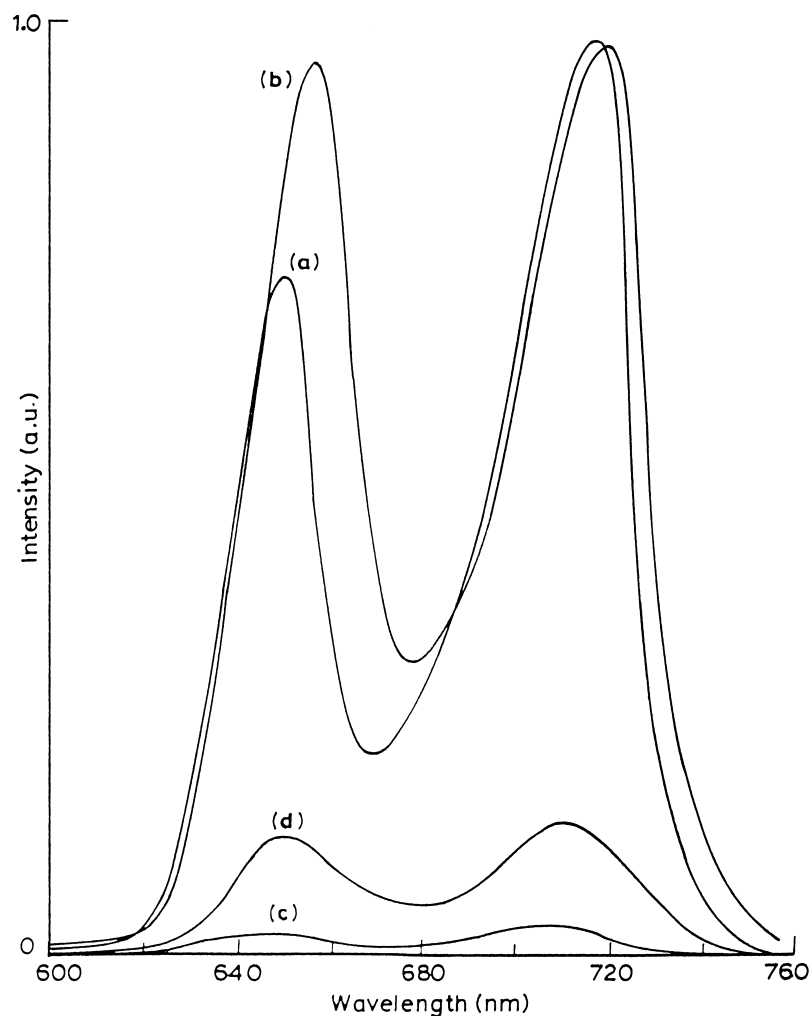


Fig. 4. Fluorescence spectra ( $\lambda_{ex}$  = 510 nm) of free-base fluoroarylporphyrin–quinones (a) H<sub>2</sub>1a, (b) H<sub>2</sub>1b, (c) H<sub>2</sub>2a, and (d) H<sub>2</sub>2b in CH<sub>2</sub>Cl<sub>2</sub> solution at 300 K.

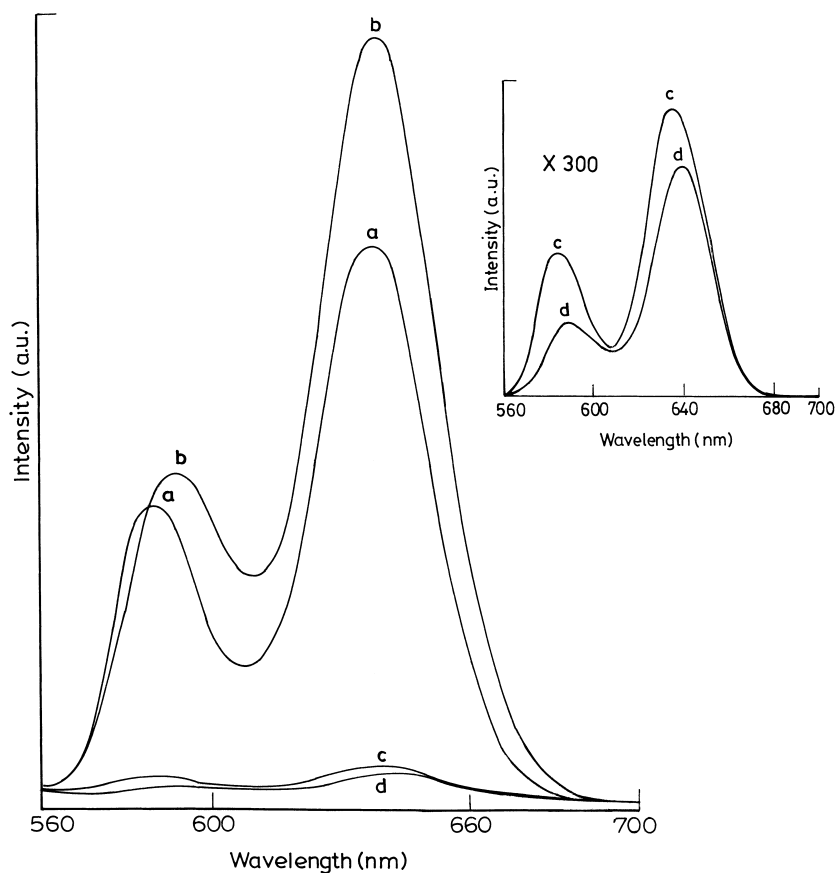


Fig. 5. Fluorescence spectra ( $\lambda_{\text{ex}} = 540 \text{ nm}$ ) of zinc(II) derivatives of the fluoroarylporphyrin-quinones (a) Zn1a, (b) Zn1b, (c) Zn2a, and (d) Zn2b in  $\text{CH}_2\text{Cl}_2$  solution at 300 K. Inset shows the spectra of porphyrin-quinones in expanded scale.

escence was observed for all the porphyrin-quinones. It is of interest to note the  $\beta$ -pyrrole-substituted tetraphenylporphyrin-benzoquinone ( $\text{H}_2\text{2d}$ ) exhibit very weak fluorescence in dichloromethane solution similar to that observed for the *meso*-substituted triphenylporphyrin-quinone ( $\text{H}_2\text{2c}$ ). The quenching of fluorescence in these porphyrin-quinone systems is ascribed to the efficient electron transfer from porphyrin to the quinone moiety upon photoexcitation. It is found that the fluoroarylporphyrin-quinones are relatively more fluorescent in contrast to the tri/tetraphenylporphyrin-quinone systems. The fluorescence quantum yields of  $\text{H}_2\text{2a}$  and  $\text{H}_2\text{2b}$  are found to be solvent dependent (Table 4), the fluorescence quenching being more in solvents of higher dielectric constant compared to those found in the solvents of lower dielectric constants. The data on the fluorescence behaviour of the porphyrin-quinone systems can be understood on the basis of the Fig. 6. In accordance with the scheme in Fig. 6, the deactivation route via a charge-separated state will be more effective, the more solvent is the polar [23]. The stabilisation of the charge-separated state with increasing the solvent polarity indicates that an electron-transfer mechanism is involved. An analysis of the data in Table 4 showed that there was a substantial decrease in the relative quantum yield values for the  $\text{H}_2\text{2a}$  in going from less polar *n*-hexane to the solvents of higher

polarity. A similar behaviour was observed for  $\text{H}_2\text{2b}$ . It is worthy to mention here that  $\text{H}_2\text{2a}$  exhibits higher fluorescence quantum yield in *n*-hexane while in solvents of higher polarity  $\text{H}_2\text{2b}$  shows higher fluorescence quantum yields though  $\text{H}_2\text{2b}$  has more favourable free-energy for electron transfer than  $\text{H}_2\text{2a}$  by  $\approx 50 \text{ meV}$ .

We carried out time-resolved fluorescence studies with the synthesized porphyrins. The free-base *meso*-phenylporphyrin-quinones and the zinc(II) derivatives of the porphyrin-quinones exhibit very weak fluorescence. Time-resolved fluorescence data on the free-base *meso*-fluoroarylporphyrin-quinone systems and their zinc(II) derivatives

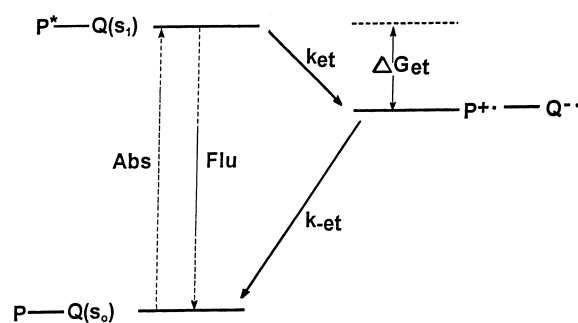


Fig. 6. Photoinduced electron-transfer scheme of the porphyrin-quinones.

Table 4  
Photophysical data <sup>a</sup> of fluoroarylporphyrin–quinones and their zinc(II) derivatives in different solvents <sup>b</sup> at 300 K

Compound	1	2	3	4	5
<b>H<sub>2</sub>2a</b>	644,711(1.0)	647,711(0.05)	643,711(0.03)	646,708(0.12)	644,704(0.02)
$\tau_1$ (ns) <sup>c</sup>	0.08(0.16)	0.12(0.96)	0.13(0.97)	0.21(0.86)	0.23(0.87)
$\tau_2$ (ns)	6.23(0.84)	9.39(0.04)	7.53(0.03)	8.06(0.14)	8.16(0.13)
$\Delta G_{ET}$ (meV) <sup>d</sup>	–123	–162	–350	–390	–397
$k_{ET}$ (s <sup>–1</sup> )	$1.17 \times 10^{10}$	$8.23 \times 10^9$	$7.5 \times 10^9$	$4.55 \times 10^9$	$4.23 \times 10^9$
<b>H<sub>2</sub>2b</b>	652,711(1.0)	651,712(0.50)	654,710(0.37)	650,711(0.55)	647,708(0.34)
$\tau_1$ (ns) <sup>c</sup>	0.69(0.86)	0.55(0.18)	0.28(0.37)	109(0.19)	0.24(0.80)
$\tau_2$ (ns)	7.66(0.14)	8.78(0.82)	7.90(0.63)	9.09(0.81)	6.43(0.20)
$\Delta G_{ET}$ (meV) <sup>d</sup>	–268	–307	–495	–535	–542
$k_{ET}$ (s <sup>–1</sup> )	$1.32 \times 10^9$	$1.72 \times 10^9$	$3.39 \times 10^9$	$8.08 \times 10^8$	$4.06 \times 10^9$
$\Phi_{H_22a}/\Phi_{H_22b}$ <sup>e</sup>	1 : 0.27	1 : 2.86	1.349	1 : 1.18	1 : 6.42
$\Phi'H_22a/\Phi'H_22b$ <sup>f</sup>	1 : 0.25	1 : 17.65	1 : 13.76	1 : 13.76	1 : 5.221 : 1.50
<b>Zn2a</b>					
$\tau_1$ (ns) <sup>c</sup>	0.17(0.91)	0.34(0.35)	0.77(0.50)	0.31(0.48)	0.06(0.99)
$\tau_2$ (ns)	1.70(0.09)	1.66(0.65)	1.77(0.50)	1.75(0.52)	2.32(0.01)
$k_{ET}$ (s <sup>–1</sup> )	$5.29 \times 10^9$	$2.38 \times 10^9$	$7.33 \times 10^{10}$	$2.65 \times 10^9$	$16.2 \times 10^9$
<b>Zn2b</b>					
$\tau_1$ (ns) <sup>c</sup>	0.28(0.72)	0.61(0.41)	0.07(0.67)	0.48(0.50)	0.08(0.93)
$\tau_2$ (ns)	1.73(0.28)	1.76(0.59)	2.05(0.33)	1.92(0.50)	2.05(0.07)
$k_{ET}$ (s <sup>–1</sup> )	$2.99 \times 10^9$	$1.02 \times 10^9$	$9.80 \times 10^{10}$	$1.56 \times 10^9$	$11.8 \times 10^9$

<sup>a</sup> The steady-state quantum yield values in parenthesis are in reference to respective porphyrin–quinones in *n*-hexane ( $\Phi = 1$ ).

<sup>b</sup> The solvents are (1) *n*-hexane, (2) toluene, (3) dichloromethane, (4) benzonitrile, (5) acetonitrile.

<sup>c</sup> The amplitudes of the lifetimes are in parenthesis.

<sup>d</sup> The corrected  $\Delta G_{ET}$  (meV) values are calculated using a mean ionic radius of  $P^{+} - Q^{-} = 5.2 \text{ \AA}$  and center-to-center distance  $6.5 \text{ \AA}$ .

<sup>e</sup> Relative quantum yield values are with reference to  $H_21a$  in *n*-hexane ( $\Phi = 1.0$ ).

<sup>f</sup> Relative quantum yields using ns lifetime data.

in five different solvents are presented here. A marginal change was observed in the singlet lifetime (single component) values for  $H_21a$  (8.1–11.0 ns) and  $H_21b$  (7.9–9.99 ns) in a wide range of polarity of the solvents. The results of time-resolved studies of fluoroarylporphyrin–quinones are shown in Table 4. It is found that there is a significant difference in singlet lifetime in changing the solvent from less polar *n*-hexane to highly polar acetonitrile. The observed fluorescence decays can be fit into bi-exponential expression with a faster lifetime component ( $\tau_1$ ) and a slower component ( $\tau_2$ ). The shorter component of the bi-exponential decay was attributed to the deactivation of the porphyrin excited state by intramolecular electron transfer to the quinone and the longer lifetime component was assigned to the decay of porphyrin–hydroquinone generated by porphyrin sensitized photoreduction [11]. The data in Table 4 show that the shorter lifetime observed for  $H_22a$  in all solvents have much larger amplitude relative to that observed for longer lifetime component. In contrast to this,  $H_22b$ , in most of the solvents exhibit higher amplitude for the longer lifetime component relative to that observed for shorter lifetime component. This reflects in the higher steady-state quantum yield values observed for  $H_22b$  over  $H_22a$  system. A similar feature is seen in the zinc(II) derivatives. It is possible to compare the relative quantum yields obtained from lifetime data with those of steady-state measurements for these free-base porphyrin–quinone systems. The zinc(II) derivatives, however, display very low quantum yields and hence no quantification of the data is

attempted here. The relative fluorescence quantum yield values were corrected for contributions from longer lived hydroquinone species using the nano second lifetime data by the expression [11],

$$\Phi' = X(\tau_1/\tau_0) + (1 - X) \quad (1)$$

where  $\Phi'$  is the relative fluorescence quantum yield,  $\tau_1$  the lifetime of the shorter component of porphyrin–quinones in different solvents,  $\tau_0$  the lifetime of the reference compound ( $H_21a$  in *n*-hexane, 8.1 ns) and  $X$  the fraction of sample in the quinone form (amplitude of shorter lifetime component). The ratio of the calculated values of relative quantum yields of fluoroaryl ( $H_22a$ ) and aminofluoroarylporphyrin–quinone ( $H_22b$ ) in different solvents are listed in Table 4. It is interesting to note that the relative ratio of the quantum yield values follow the same trends as that observed from steady-state measurement. The observed decrease in fluorescence lifetimes can be related to an electron-transfer (ET) rate constant assuming that the shorter fluorescence lifetime of the linked porphyrin–quinone molecule is due entirely to the photoinduced electron transfer. The rate constant  $k_{ET}$  is obtained by [4],

$$k_{ET} = 1/\tau_1 - 1/\tau_2 \quad (2)$$

and the values are shown in Table 4. The data in Table 4 revealed that the rate of photoinduced electron transfer in  $H_22a$  is higher than that of  $H_22b$  by a factor of 2–8 in all the solvents studied, though the former is having less favourable free energy for electron transfer than the later. Attempts to

correlate the fluorescence quenching and rate data with  $\Delta G_{ET}$  in these systems using Marcus relationship [24,25] for electron transfer have not yielded satisfactory results. In addition, the fluorescence data and the rate of photoinduced electron transfer in these fluoroarylporphyrin–quinone molecules correlate poorly with solvent polarity. A possible reason for this behaviour lies in the limitations to make accurate determinations of the true energetics [26]. In short distance rigid donor–acceptor molecules the opposite charges separate to a fixed distance and the energy of the product state is differentially lowered by the columbic energy whereby large dielectric solvents shield the charges more effectively than non-polar solvents. Dielectric relaxation of solvents also contribute for the poor correlation with solvent polarity [27]. The dependence of temperature, viscosity and the dielectric relaxation on the rates of photoinduced electron transfer in these systems are in progress.

### Acknowledgements

The authors thank the Department of Science and Technology, Government of India, New Delhi for financial support. We also thank Prof. Periasamy and Dr. N.C. Maity of T.I.F.R., Mumbai for lifetime measurements.

### References

- [1] J.S. Connolly, J.R. Bolton, Photoinduced Electron Transfer, in; M.A. Fox, M. Channon (Eds), Elsevier Publishers, Amsterdam, Part D, 1988, p. 303.
- [2] H. Kurreck, M. Huber, *Angew. Chem. Int. Ed. Engl.* 34 (1995) 849.
- [3] D. Gust, T.A. Moore, P.A. Liddell, G.A. Nemeth, L.R. Makings, A.L. Moore, D. Barrett, P.J. Pessiki, R.V. Bensanon, M. Rougee, C. Chachaty, F.C. De Schryver, M.V. Auweraer, A.R. Holzwarth, J.S. Connolly, *J. Am. Chem. Soc.* 109 (1987) 846.
- [4] M.R. Wasielewski, *Chem. Rev.* 92 (1992) 43.
- [5] Y. Sakata, H. Tsue, M.P. O'Neil, G.P. Wiederrecht, M.R. Wasielewski, *J. Am. Chem. Soc.* 116 (1994) 6904.
- [6] J. Rodriguez, C. Kirmaier, M.R. Johnson, R.A. Friesner, D. Holten, J.L. Sessler, *J. Am. Chem. Soc.* 113 (1991) 1652.
- [7] B.A. Leland, A.D. Joran, P.M. Felker, J.J. Hopfield, A.H. Zewail, P.B. Dervan, *J. Phys. Chem.* 89 (1985) 5571.
- [8] K. Wynne, S.M. LeCours, C. Galli, M.J. Therien, R.M. Hochstrasser, *J. Am. Chem. Soc.* 117 (1995) 3749.
- [9] K. Kamioka, R.A. Cornier, T.W. Lutton, J.S. Connolly, *J. Am. Chem. Soc.* 114 (1992) 4414.
- [10] M.A. Bergkamp, J. Dalton, T.L. Netzel, *J. Am. Chem. Soc.* 104 (1982) 253.
- [11] A.D. Joran, B.A. Leland, P.M. Felker, H.J. Zewail, J. Hopfield, P.B. Dervan, *Nature* 327 (1987) 508.
- [12] M.R. Wasielewski, M.P. Niemczyk, W.A. Svec, E. Bradley Pewitt, *J. Am. Chem. Soc.* 107 (1985) 1080.
- [13] J.S. Lindsey, R.W. Wagner, *J. Org. Chem.* 54 (1989) 828.
- [14] A. Sen, V. Krishnan, *Tetrahedron Letts.* 37 (1996) 8437.
- [15] A. Sen, V. Krishnan, *Tetrahedron Letts.* 37 (1996) 5421.
- [16] T. Elangovan, V. Krishnan, *Chem. Phys. Lett.* 194 (1992) 139.
- [17] N. Periasamy, S. Doraisamy, G.B. Maiya, B. Venkatraman, *J. Chem. Phys.* 98 (1988) 1638.
- [18] G.B. Dutt, S. Doraisamy, N. Periasamy, B. Venkatraman, *J. Chem. Phys.* 93 (1990) 9498.
- [19] A. Sen, V. Krishnan, *J. Chem. Soc., Faraday Tans.* 93 (1997) 4281.
- [20] S. Rao, V. Krishnan, *J. Molecul. Struct.* 329 (1994) 279.
- [21] R.A. Cornier, M.R. Posey, W.L. Bell, H.B. Fonda, J.S. Connolly, *Tetrahedron* 45 (1989) 4831.
- [22] A.Z. Weller, *Phys. Chem. (Wiesbaden)* 113 (1982) 93.
- [23] H.A. Staab, G. Voit, J. Weiser, M. Futscher, *Chem. Ber.* 125 (1992) 2303.
- [24] R.A. Marcus, *J. Chem. Phys.* 24 (1956) 966.
- [25] R.A. Marcus, N. Sutin, *Biochim. Biophys. Acta.* 811 (1985) 265.
- [26] M.D. Archer, V.P.Y. Gadzekps, J.R. Bolton, J.A. Schmidt, A.C. Weedon, *J. Chem. Soc., Faraday Tans.* 2. 82 (1986) 2305.
- [27] E.M. Kosower, D. Huppert, *Ann. Rev. Phys. Chem.* 37 (1986) 127.